

Application of electrical resistivity tomography (ERT) survey for investigation of the landslide: a case study from Taprang landslide, Kaski district, west-central Nepal

Ashok Sigdel* and Radha Krishna Adhikari

*Department of Geology, Tri-Chandra Multiple Campus,
Tribhuvan University, Kathmandu, Nepal*

**Corresponding author's email: ashoksigdel80@gmail.com*

ABSTRACT

The depth of the slip surface and thickness of the overburden deposit play a major role in assessing the slope stability of a landslide. Electrical Resistivity Tomography (ERT) survey was carried out in the Taprang Landslide, Kaski district, west-central Nepal to determine subsurface lithological conditions, depth and geometry of the slip surface. Wenner and dipole-dipole arrays were mainly applied in this ERT survey. The electrical resistivity survey revealed that there is a wide range of resistivity value which shows different kinds of layers in the subsurface, and the boundaries between these layers played a significant role to identify the slip surface. The data show mainly three layers from surface to bottom. An upper layer represents the dry to saturated colluvium and sandy gravelly soil (500 to 8000 Ωm), the middle layer is highly saturated soil with low resistivity value (100–700 Ωm) and unweathered fresh bedrock of schist and quartzite with high resistivity value (1000 to 8000 Ωm) at the bottom layer. The slip surface is considered as depth 25 m at the crown, 10–20 m at the main body part, and below 50 m at the toe and curved in geometry which indicates the rotational type of landslide. Investigation of the slip surface in a landslide using the ERT survey aids to know the slope stability.

Keywords: Electrical resistivity tomography; Slip surface; Taprang landslide

Received: 20 April, 2020

Received in revised form: 28 August, 2020

Accepted: 29 August, 2020

INTRODUCTION

Application of the Electrical Resistivity Tomography (ERT) survey has been increasing for many years and acts as a most significant geophysical technique in investigating of the landslide (Drahor et al., 2006, Coskun et al., 2015). Electrical resistivity of the materials is a criterion showing a wide range of values, which is sensitive to several factors such physical properties of the materials (soil type, porosity, permeability etc.), volume and conductivity of the water, and weathering and fracturing of the bedrock (Telford et al., 1990; Jongmans and Garambois, 2007; Ponzianietal., 2011; Epada et al., 2012). The geophysical method such as ERT can provide 2D or 3D models of the subsurface layers of the materials in the landslide for studying the slope (Suzuki and Higashi 2001; Lapenna et al., 2003, 2005). It is also useful to determine the mechanical properties of the soil, characteristics of the slip surface, and groundwater condition (Bogoslovsky and Ogilvy, 1977; Sassa et al., 2018). The depths of the slip surface and water table condition can be studied by the geophysical methods (Caris and Van Ash, 1991). The geophysical technique can be used for knowing the internal structure and the mechanical properties of a soil or rock mass to assess the slope stability of a landslide (Hack 2000). The combined investigation of geophysical

surveys, field observation, and geotechnical studies become a reliable tool for the study of instability of slope (Havenith et al., 2000, Yang et al., 2004). The electrical tomography method is useful for studying landslides and evaluating the risk and hazard together with delimiting the potentially unstable overlying deposits (Batayneh and Al-Diabat 2002). Bichler et al. (2004) mentioned that the electrical resistivity survey can be used as the primary tool for mapping to know the electrical resistivity contrasts, geometry, and depth of different layers. Similarly, the study of geological features in a landslide by using the geophysical method provides an useful technique (Konagai et al., 2005). Asriza et al. (2017) used the ERT survey and other laboratory analyses to identify the location of the slip surface for the stability of a landslide. The variation of apparent resistivity in-depth-wise and identifying the saturated zone was investigated by the ERT survey (Kim et al., 2009). Similarly, Panta (2001) used several geophysical methods to know the subsurface information regarding the type of materials, depth to water table and bedrock, slip surface, and displaced masses of the landslides of Nepal.

Landslides in Nepal are very frequent and distributed in different parts which are very active during the rainy season. These active landslides caused several damages of land, forest, and houses as well as human death for

many years. Hence, the detailed characteristics of the active landslide are very necessary to know mitigation measures to save lives immediately in Nepal. To date, causes and mechanisms of the landslide have been studied based on geomorphic, engineering geological, and geotechnical aspects with limited subsurface boreholes data. Still, a geophysical survey such as ERT is rarely applied for investigation of a large landslides in Nepal. Therefore, this study has tried to fulfill this lacking methodology such as the ERT survey in an active Taprang landslide in Kaski district as a case study. The development of Taprang landslide generates a huge amount of damage and even loss of lives and properties. This landslide also placed the people in Kaski, Lamjung, and Tanahu districts by damming the Madi River (Khanal et al., 2013). In the past, except for some engineering geological and clay mineralogical studies (Khanal et al., 2013; Regmi et al., 2017), no geophysical survey was applied to such a slide. Therefore, the main purpose of this study is to carry out the ERT survey with the objectives of mapping its subsurface geological, hydrogeological, depth and geometry of slip surface of the Taprang landslide.

STUDY AREA

Taprang landslide is located in the Madi Rural

Municipality ward no. 6 at Kaski district (Fig. 1). The maximum elevation is 1700 m at its crown along the sickles road and the minimum elevation is 1015 m at its toe. The geographical coordinate of the landslide is between 28° 18' 84.49" to 28°18'34.24" N and 84° 04' 24.93' to 84° 05' 23.75" E. The slope angle of the landslide covered area ranges from 10° to 60°, and very steep at the main body part of the landslide. The length of this huge and largest landslide is about 1700 m from toe to crown. The landslide covers about 673,950 m². A main drainage and other small tributaries are flowing through the landslide and finally join to the Madi River.

GEOLOGICAL SETTING

Geologically, the Taprang landslide lies in the Ghanpokhara Formation of the Lesser Himalaya zone (DMG, 1983). The Ghanpokhara Formation consists of black carbonaceous shale, slate, phyllite, and schist with white dolomitic limestone. Dhital (2015) described the geology of the area and included in slate, shale, sandstone, siltstone, and graphitic schist unit of Lesser Himalayan sequence. These units are correlated with the Nawakot Complex in central Nepal, Lesser Himalaya by after Stöcklin and Bhattarai (1977). The Lesser Himalayan zone is separated from the Higher Himalayan zone by the Main Central Thrust (MCT).

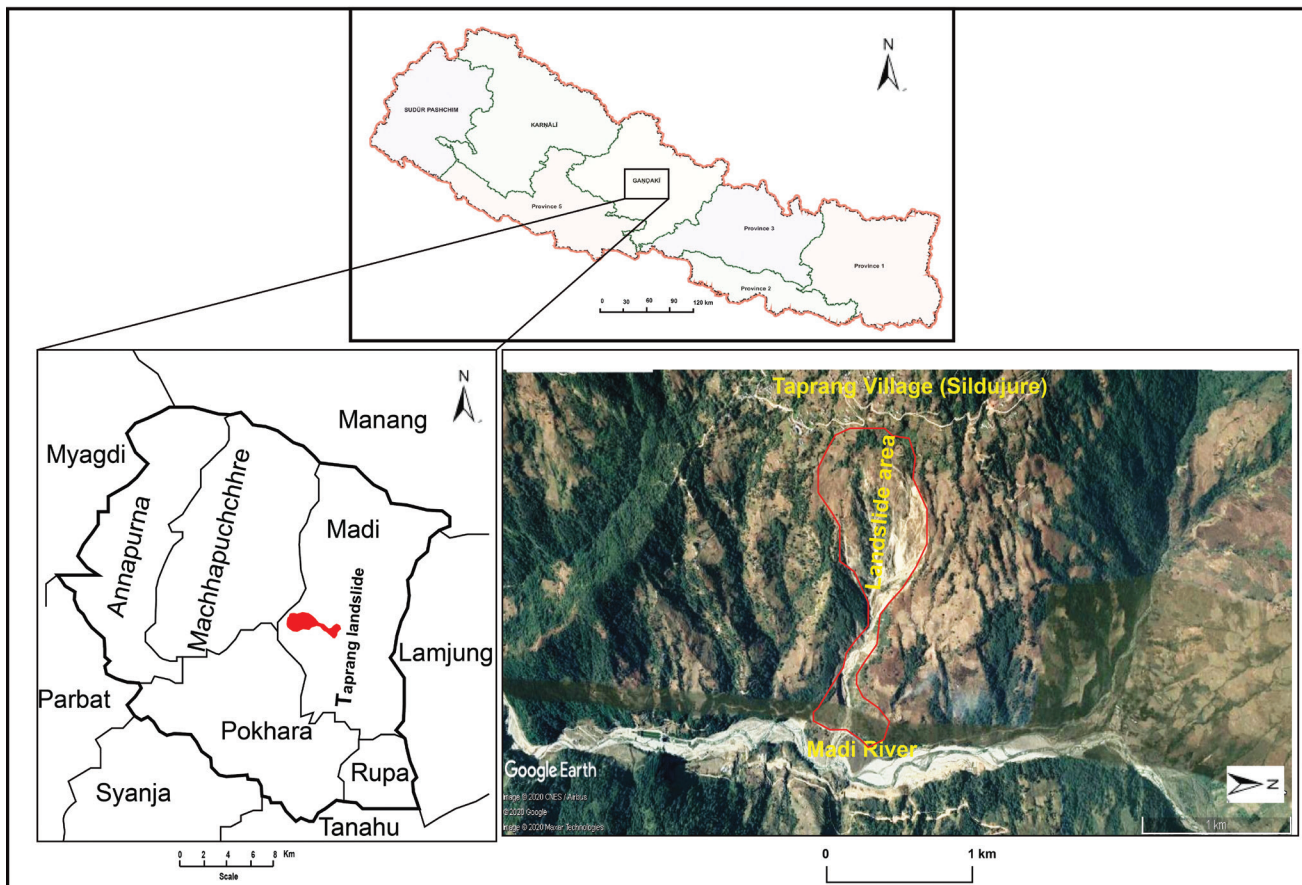


Fig. 1: Location map of the study area.

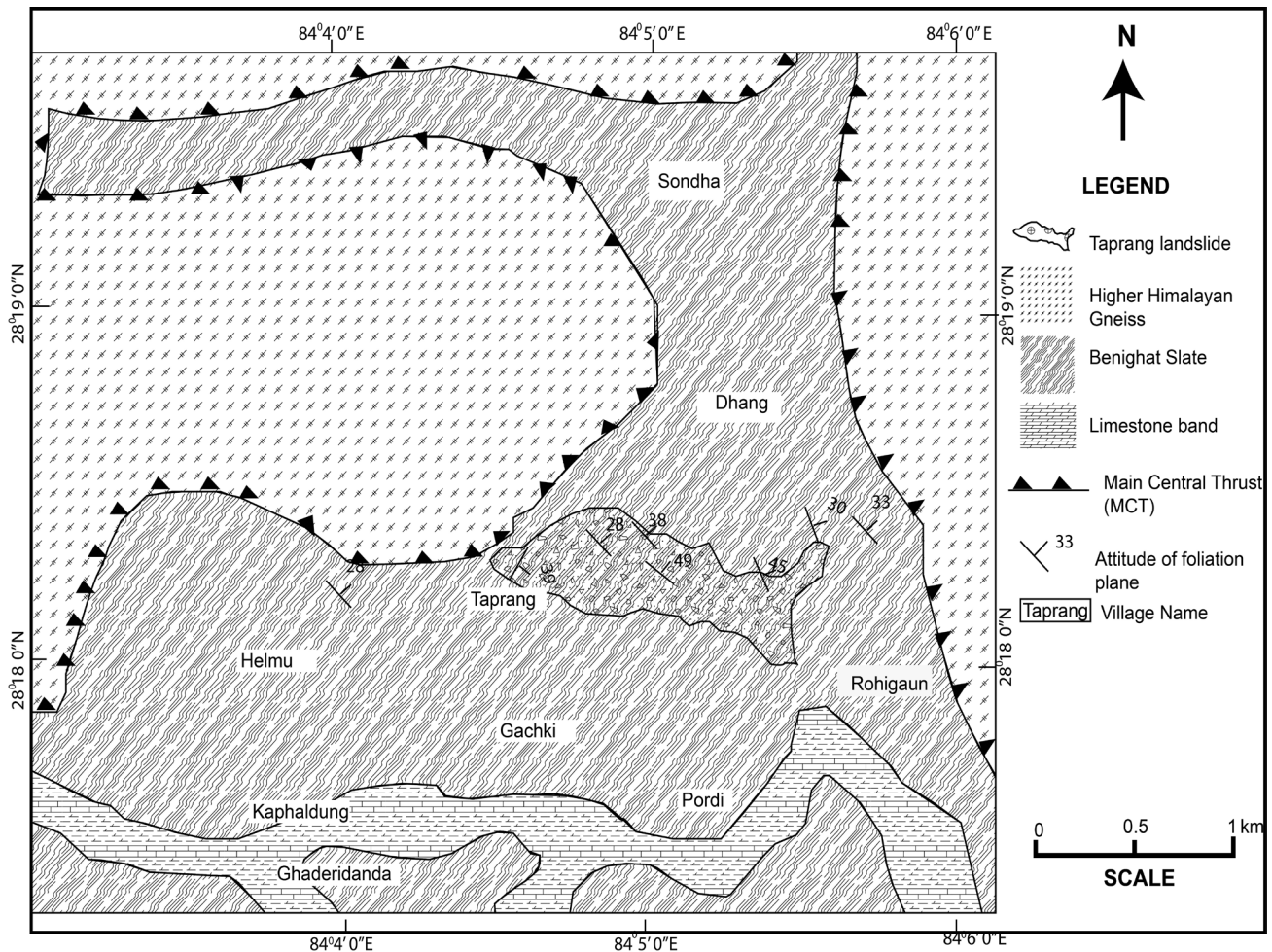


Fig. 2: Generalized Geological Map of the Landslide Area (modified from Regmi et al., 2017).

The MCT passes from the upper part of the crown in the landslide area. Schist and gneiss are the main lithology of the Higher Himalayan zone which consists of high-grade minerals such as sillimanite, kyanite, garnet, biotite, feldspar, muscovite, and quartz (Dhital 2015). Regmi et al. (2017) also studied the detailed geology of the Taprang landslide and consists of grey to black, thinly laminated, highly foliated schist which is somewhat intercalated with thinly bedded, white to grey colored quartzite (Fig. 2). The exposed rock is highly weathered, grey, coarse-grained, thickly schist with persistent foliation joint. Several quartz veins are also developed around the schist unit. The representative attitude of the foliation plane is $N30^{\circ}W/37^{\circ}NE$. The dip amount of the bedrock ranges from 25° – 40° throughout the landslide slope. This unit is correlated with Benighat slate and its equivalent of the Nawakot complex of Central Nepal (Regmi et al., 2017).

CHARACTERISTICS OF THE LANDSLIDE

The landslide comprising mainly of thick colluvium deposits and residual soil. The landslide is a complex

type of slide consisting of the combination of several types of slides such as slide, fall, and flow. Few other small scale slides are also present within this landslide. The detailed morphology and characteristics of the landslide are shown in Figure 3.

The crown is mainly extended towards the left flank of the landslide where mainly residual soil is present. The residual soil and the colluvium are the main lithology at the crown area. A large scrap is present at these places. The damaged school building and a small temple with cracked walls are present in the crown area (Fig. 4a). The slope angle of the crown to the main body part is 30° – 32° . Several cracks are also present at the crown part. The observed length of the cracks range from 1–3 m and depth up to 1 m.

The main body of the landslide is covered by thick and very loose colluvium which consists of pebbles, cobbles and boulders of schist, and quartzite having 1–5 mm in diameter. Several tensional cracks and vertical cracks are also observed throughout the middle part of the landslide area. The length of the cracks ranges from 1–5 m and depth up to 2 m. The bedrock of schist and quartzite are visible in the

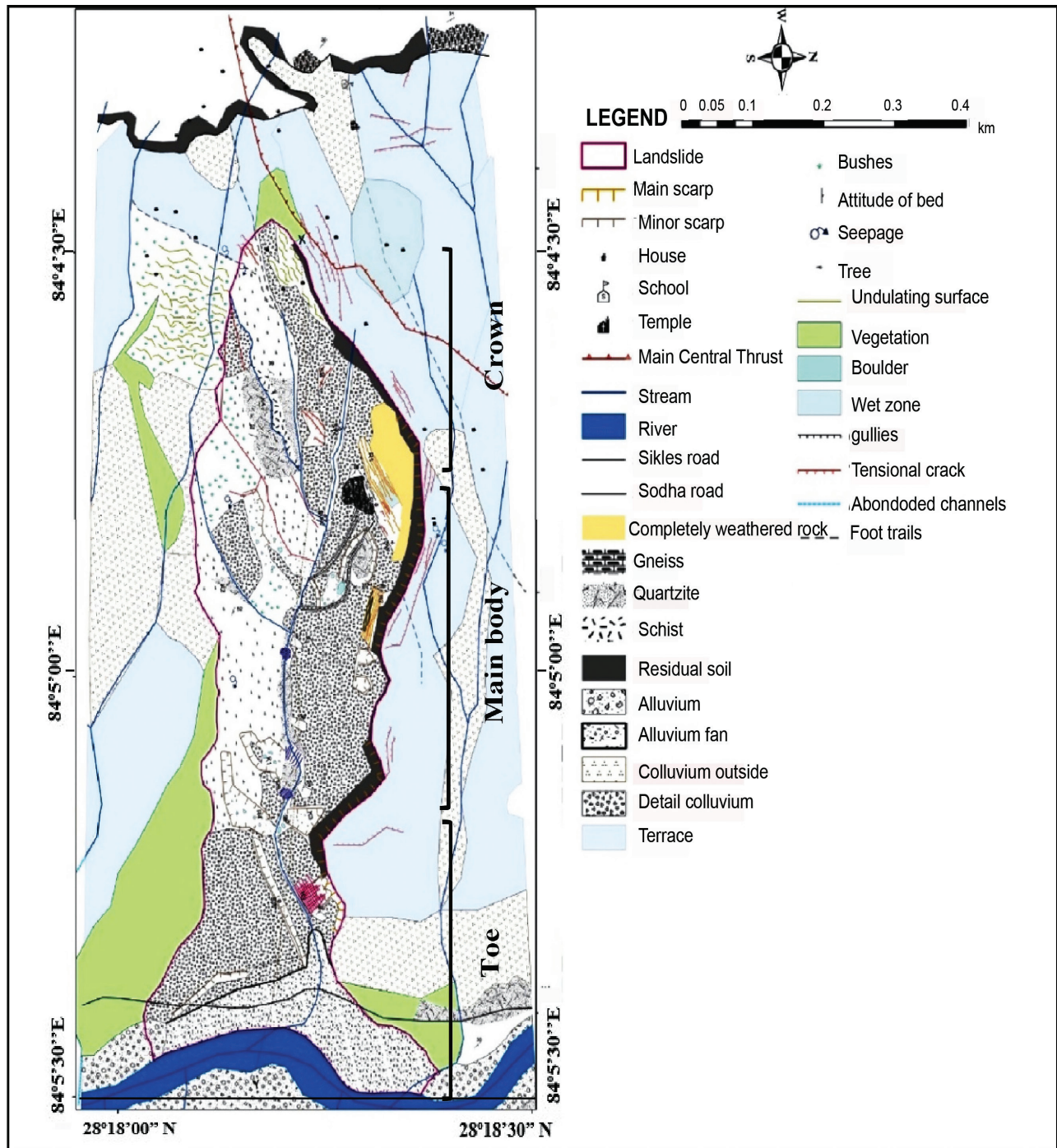


Fig. 3: Morphological map of the Taprang landslide.

outcrop in some places which is highly weathered, fractured, and jointed and attached to the colluvial mass. A small scarp of the bedrock is observed just end of the middle part of the landslide which mainly comprises with highly weathered schist. Some debris of rock is also present in this area (Fig. 4b)

The slope is about 40° towards the toe area. Several seepage zones are observed within the upper and middle parts of the area which may be due to the percolation of water from hill slope. The land use of the main part of the slide is grassland and forest in the right flank of the landslide. At the left flank,

paddy and cultivated land are present which caused large scarp is developed and the soil is loosened by the infiltration of water (Figs. 4c and 4d).

At the toe of the landslide, mainly colluvium and debris deposits are present which are carried by the small streams and active slide along the left flank of the landslide. The colluvium and debris of the toe consist of thick deposits of pebbles cobbles and boulders with soil (Figs. 4e, 4f). The width of the toe is more than 100 m. The slope angle is about 5–10°. Besides this, highly weathered and fractured bedrock of schist is present nearby the toe.



Fig. 4: (a) Cracks on the temple are present in the crown part (b) Large scrap present at the main body (c) Active part of the landslide at the left flank of the body (d) Several gullies and seepage are present at the main body (e) Downslope view of the toe and (f) Thick debris and overall landslide view from the toe area.

METHODOLOGY

To recognize subsurface geological information, geophysical investigation (ERT) was carried out. The ERT methodology consists of the measurement of a series of direct current (DC) electrical resistivity along with the profile of more than 300 m. The

stainless steel electrodes are used and placed at a uniform distance of about 5 m intervals, which is adopted in this study. The measurement is automatic and programmed in the software which is used for selected different array (Pasierb, 2012; Loke, 2014). The depth of the layer depends on the lateral distance of the profiles such as the increase in the

spacing increases the depth. Generally, 1/3–1/5 of the depth is taken for data processing (Wightman et al., 2003). Wenner and dipole-dipole arrays are applied in this study due to their high depth penetration and the horizontal resolution (Loke, 2009; Kneisel and Hauck, 2008). The instruments used during the ERT survey are Multi-function digital DC Electrical Resistivity (GD-10, Geomative), Multiplex electrode converter (Multi-electrode switching equipment CS 60), Multicore cables with each takes out at every 5 m and Battery with 144 volts. The data processing of the ERT survey was carried out by two-dimensional RES2DINV software (Geotomo Software, Loke, 2009, 2014). The applied arrays in this ERT survey are shown in Fig. 5. In the Wenner array, the current and potential electrode pairs have a common mid-point. The outer two electrodes (A and B) are the current electrodes (source) and the inner two electrodes (M and N) are the potential electrodes (receiver). The distance between both current and potential electrodes is the same as a .

Similarly, in the dipole-dipole array, all four electrodes are fixed in the line at measurable distances from each other. In this array, both current electrodes are next to each other at a distance a , while the potential electrodes are also next to each other at distance a and separated from the current electrode pair at a distance na .

In this study, seven profiles were carried out for the ERT survey (Fig. 6). The layout of Profile 1 was carried out 300 m length and depth is estimated about 56 m across the crown area. Profile 2 of 300 m length, which is along the crown of the landslide and estimated depth is about 56 m. Similarly, profiles 3, 4, and 5 lie in the main body of the landslide which are across, along with and across the landslide of length 300 m, respectively. Profiles 6 and 7 lie in the left flank of the toe of the landslide which is a very active part of the near toe of length 300 m. The total estimated depth of the subsurface information is 56–70 m. The electrodes spacing for all profiles is 5 m.

RESULTS

The 2D model sections obtained from data inversion are presented as resistivity tomograms (Fig. 7). These tomograms show the variation of modeled electrical resistivity in-depth and along the line of investigation. These sections illustrate an extremely heterogeneous structure both vertically and horizontally. There are low and high resistivity zones in these sections. Zones of relatively low resistivity within the body of landslide are described with the content of clayey, silty, sandy

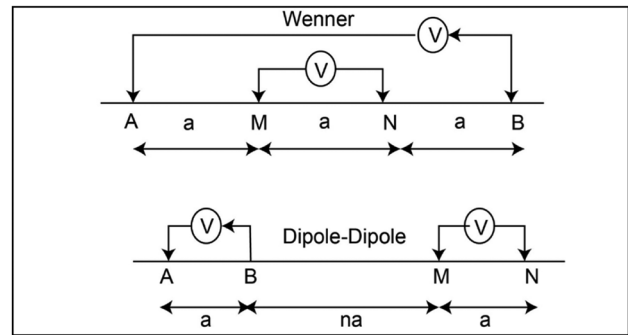


Fig. 5: General electrodes configuration of ERT survey (Griffiths and Turnbull 1985; Loke and Barker 1996).

materials, and moisture contents and high resistivity value indicates either boulders, gravels, or bedrocks as shown standard resistivity value in Fig. 8. The resistivity values of proper landslide location slightly vary from the standard value which is due to different noise of data, saturation condition, weathering, and fracturing of rock and minerals contained in the rock and soils, etc. In this, the boundary between very low and high resistivity values of lithological layers is considered as the slip surface.

Profile 1 consists of three distinct layers from surface to bottom. Upper Layer contains dry to partly saturated colluvium which has the resistivity value ranges from 1500 to 6000 Ωm . The depth of this colluvium is about 10 m from the surface. This soil probably originated from slide mass. A saturated zone with clay and the sandy layer is present from depth 10–25 m from the surface of resistivity value ranges from 100–700 Ωm . This layer marks the boundary between overburden and bedrock i.e. slip surface. At 25 m, the slip surface is present just below the saturation zone. The second layer consists of fractured bedrock of gneiss and found to extend to a depth 56 m and below from the surface which have resistivity value ranges from 2000–3000 Ωm (Fig. 7a).

Profile 2 consists of dry colluvium with sandy soil with resistivity 1000–2000 Ωm . The depth of this colluvium is about 10 m from the surface. Partly saturated soil is present from depth 10 m to 20 m from the surface (400–1000 Ωm). This layer marks the boundary between overburden and bedrock i.e. slip surface. The slip surface found at depth of 10–20 m from the surface. Below this slip surface, highly fractured to sound bedrock of gneiss is present to a depth 56 m and below. The resistivity value of this layer ranges from 1500–6000 Ωm (Fig. 7b).

Profile 3 contains dry colluvium which consists of pebbles, cobbles, and boulders with resistivity value range from 2000–8000 Ωm . The depth of this colluvial layer varies from 10–20 m. A saturated zone

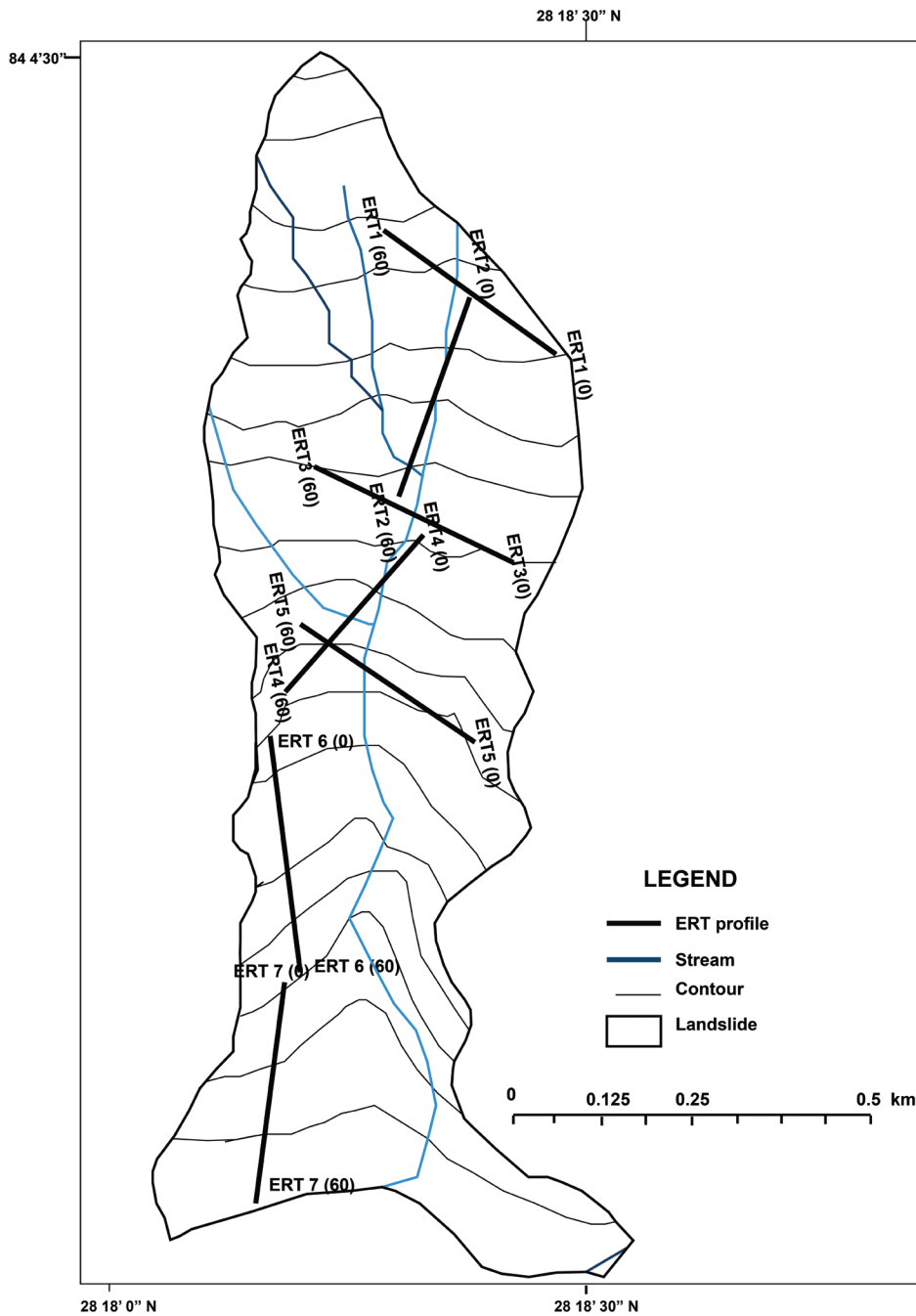
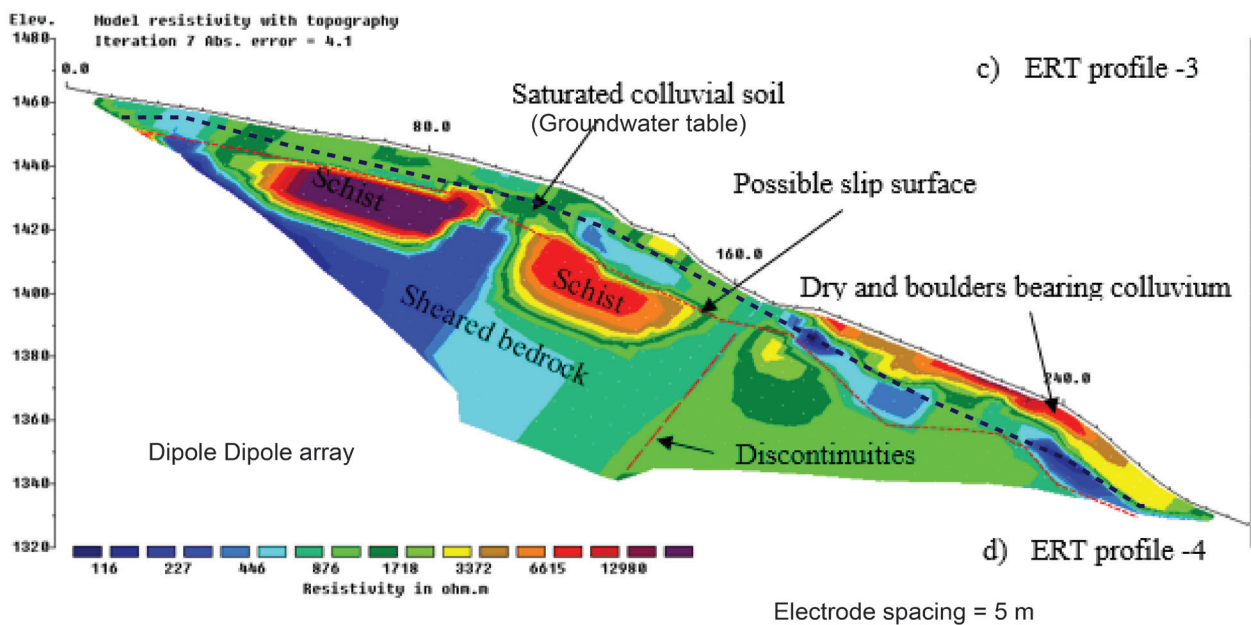
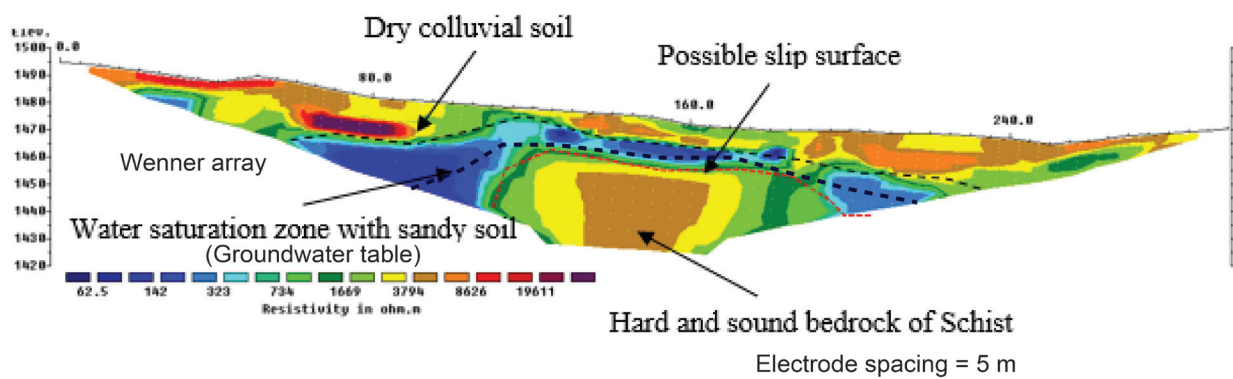
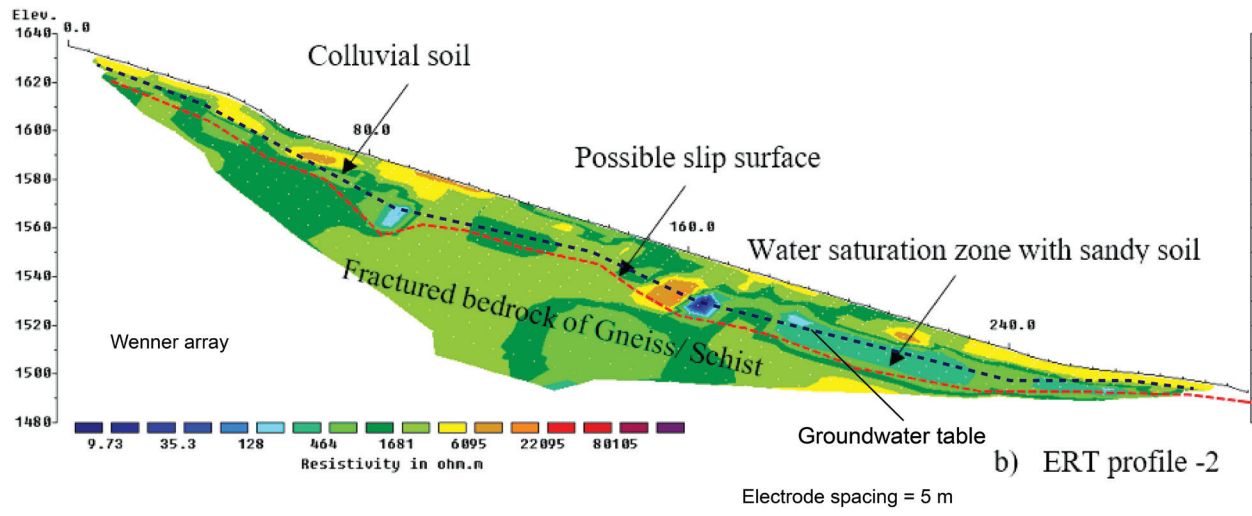
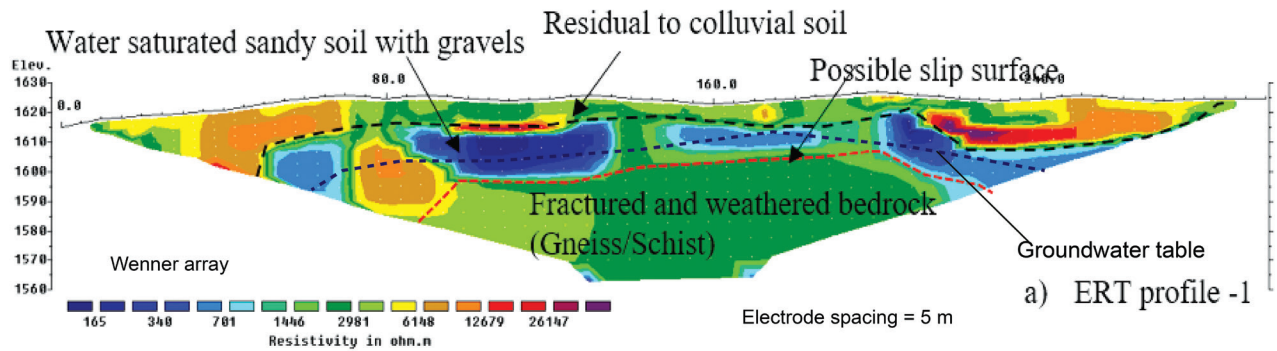


Fig. 6: Location map of the ERT profiles in Taprang Landslide.

is present below 20 m from the surface with resistivity 50–300 Ω m. This may represent the highly porous or fractured bedrock or converted into the soil stage. This layer extends below depth up to 30 m and it shrank at the center and again expands towards right flank which is seen in the tomogram. At 20–30 m below surface, there is a boundary between the top saturated zone and bedrock which represents the slip surface. The second layer consists of sound and good bedrock of schist and extends up to depth 56 m with resistivity 2000–8000 Ω m (Fig. 7c).

Profile 4 shows that thick covered saturated to dry colluvial soil is present up to depth 10 m from surface.

The resistivity of this layer ranges from 700–6000 Ω m. There is a presence of boulder-like rock patches in the central part, which may represent the bedrock of schist and quartzite which is also observed during field survey. The resistivity in this zone ranges from 3000–12000 Ω m. The depth of this layer exposed from 10–25 m below the surface. The surface where the resistivity contrast between these two layers is considered as slip surface at this point. The average depth of the slip surface is 15 m. There is the presence of structural discontinuities i.e. sheared zone in different places of this tomogram which are indicated by the presence of sheared bedrock of low resistivity value (100–500 Ω m) (Fig. 7d).



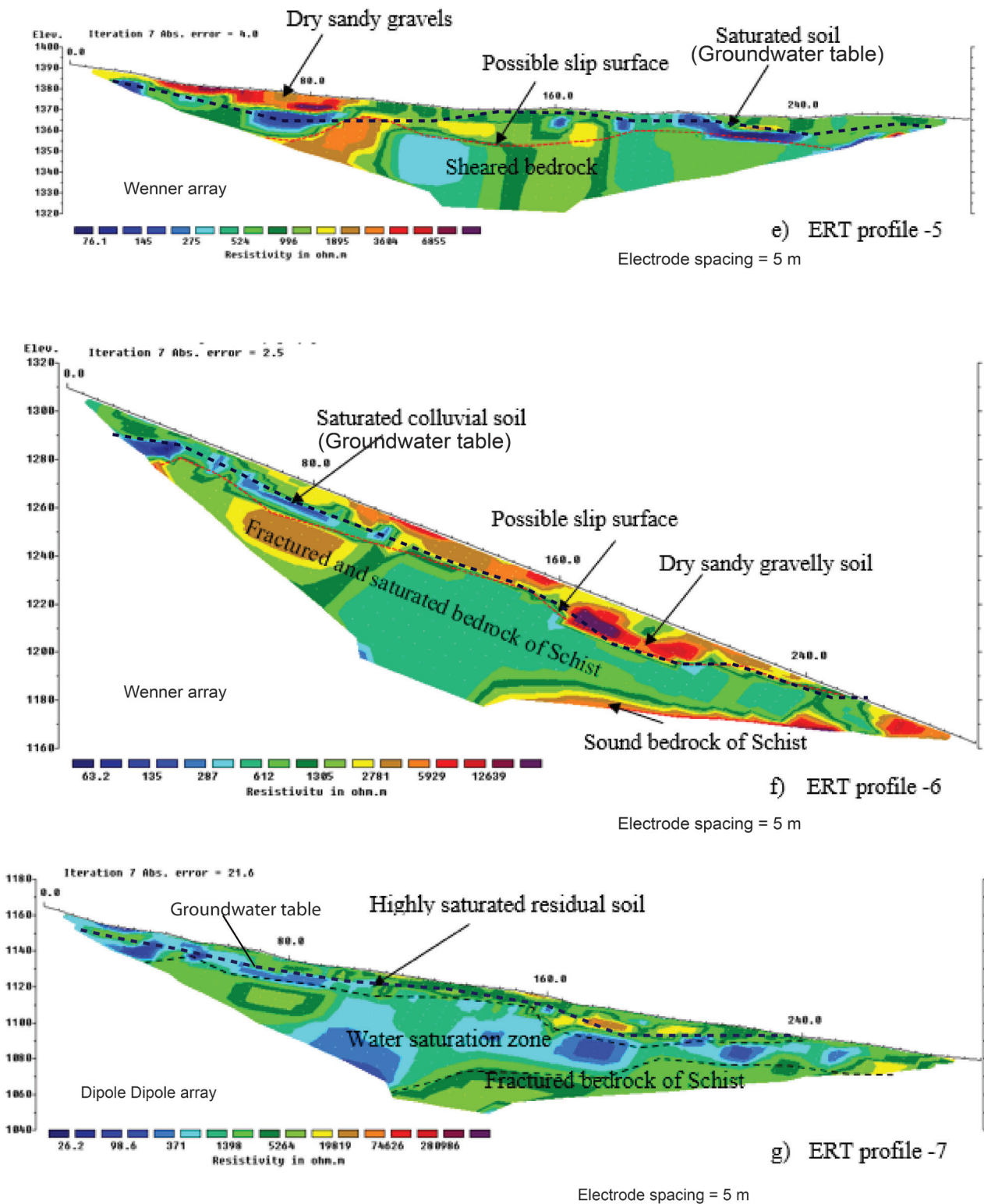


Fig. 7: Electrical resistivity tomography results (a) Profile-1 across the landslide at crown (b) Profile-2 along the landslide movement at crown (c) Profile-3, across the landslide at body part (d) Profile-4, along the landslide at body part (e) Profile-5, along the landslide at body part (f) Profile-6, along the landslide at left flank of the toe part (g) Profile-7, along the left flank of landslide at toe part.

Profile 5 consists of dry to saturated colluvium which mainly consists of boulder bearing gravels of resistivity 200–3000 Ωm. The upslope consists of dry gravels and saturated soil found towards the downslope. The depth of this colluvium extends up to 10 m from the surface. A saturated zone is present below depth 10 m

and found up to 20 m with resistivity value ranges from 70–200 Ωm. This marks the slip surface at 20 m where the boundary between the saturated layer and bedrock is encountered. The second layer consists of highly fractured, sheared, and saturated bedrock of schist, and quartzite is found to extend to a depth 56

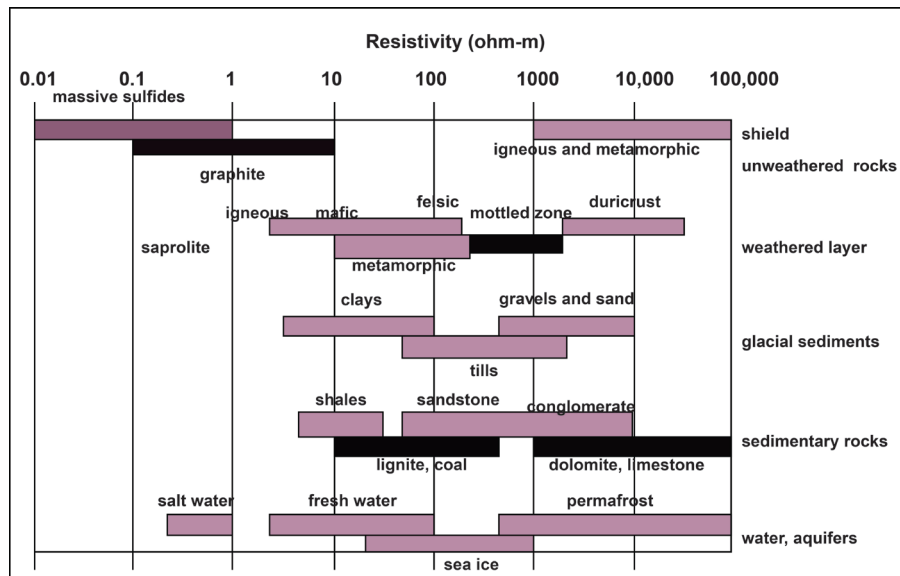


Fig. 8: Common resistivity values of earth materials (after Palacky, 1980).

m and below from the surface. The resistivity value of this layer ranges from 500–4000 Ωm (Fig. 7e).

The upper layer of the profile 6 consists of highly saturated colluvium. The depth of this colluvium ranges from 10–15 m from the surface with resistivity 500–5000 Ωm . Below this layer, low to medium resistivity, highly fractured, weathered, and porous bedrock of schist is present and found to extend to a depth from 15 to 40 m varies from places to places. The range of resistivity value is 500–3000 Ωm . High resistivity, sound bedrock of schist is present at depth 40m and extends to a depth 56 m and below from the surface which has resistivity values ranges from 2500–8000 Ωm (Fig. 7f).

The upper layer of the profile 7 consists of partly saturated residual to colluvial soil with low resistivity 20–300 Ωm . The residual soil consists of cultivated residual soil with some gravels. The depth of this layer varies at different places and present up to 5–10 m. The distinct second layer consists of a very low resistive, highly saturated, a fractured porous zone where water is flowing throughout the layer and found to extend to a depth 10–50 m from the surface. The resistivity value of this layer ranges from 100–1000 Ωm . This layer marks the boundary of bedrock and colluvium. Below this layer, highly fractured, weathered bedrock of schist is present which has resistivity value ranges from 1000–6000 Ωm (Fig. 7g).

DISCUSSION

The combined field observation and ERT tomogram sections have revealed the slip surface and characteristics of the different kinds of soil in the

landslide (Fig. 9). Colluvium mainly consisted of gravelly, sandy and silty clay characterized by wide range resistivity (500 to 8000 Ωm) which have about 10–25 m thickness in the crown part of the landslide. These colluvium probably transported from the upslope of the past landslide. A highly saturated weathered zone consisted of sandy to silty soil characterized by medium to low resistivities (100–700 Ωm) whose thickness is between 10 and 15 m. The lower resistivity value indicates the presence of the saturated condition in the unconsolidated soil while the higher values represent the dry and hard consolidated sediments (Drahor et al, 2006). The thickness of colluvium with gravelly materials are decreases towards the main body part of the landslides and the slip surface is slightly shallower than the crown part. The slip surface found to be a depth between 10–20 m from the surface. Also, the very low conductive zone between 10 m and 20 m thickness is characterized by very low resistivities (about 70–200 Ωm) represent the highly saturated sandy clay. This is interpreted as the groundwater is much shallower than the crown part. Highly saturated residual soil and colluvium found on the left flank of the landslide and slip surface is found to be deeper (about 50 m) than the crown and main body parts of the landslide. This is interpreted as the movement of the landslide is still active and colluvium materials continually deposited at the toe area as well as groundwater is continuously flowing in very shallow depth or sometime in the surface. The relatively high resistivity zones of all profile sections correspond to the block materials in the landslide body and massive bedrock formation. Fresh, sound, and unweathered zone consisted of crystalline schist and quartzite is characterized by high resistivity (1000 to 8000 Ωm).

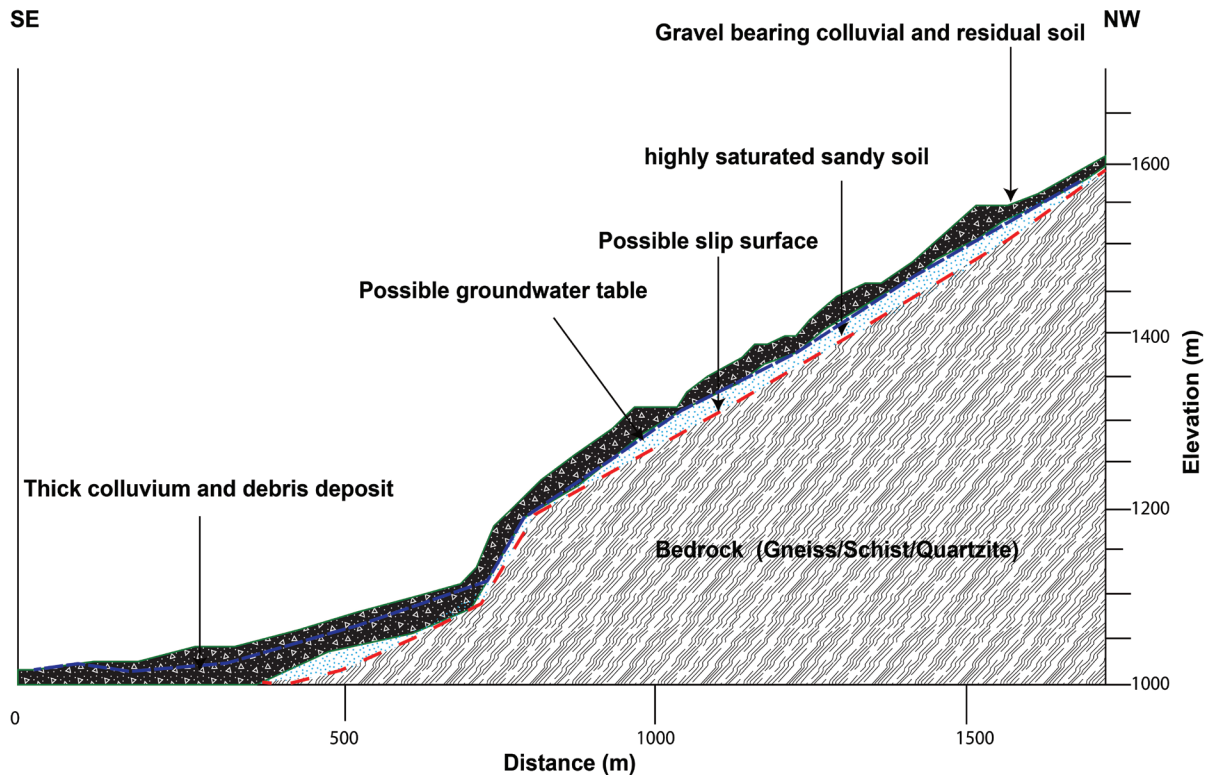


Fig. 9: Longitudinal-section of the Taprang landslide showing different lithological layer and slip surface.

The saturated sandy soil unit characterized by resistivity around $100 \Omega\text{m}$ surrounding the zone covers all of the section under the slip surface and indicates the groundwater table. The presence of groundwater just above the slip surface with low resistivity is one of the major factors for landsliding. The layer below the groundwater table can be considered as the slip surface of the landslide (Drahor et al., 2006). Hence, the boundary between upper unconsolidated deposits with low resistive groundwater table and below high resistive hard, sound and unweathered bedrock can be considered as the slip surface in this study (Havenith et al., 2000; Batayneh and al Diabat, 2002; Demoulin et al., 2003; Asriza et al., 2017). The depth of this slip surface in this landslide varying between 10 m and 30 m with average depth at 25 m at the crown and 10-20 at the main body part and more than 50 m toward the toe area. This type of geometry of the landslide is related with the topographical variation and the depth of groundwater table and this slip surface appears very similar to the rotational type and curved (Drahor et al., 2006) (Fig. 9) Hence, unconsolidated sediments above the bedrock along with several cracks and structural discontinuity such as sheared zone is present along the landslides permits easier water seepage to a deeper depth. The water flowing from the upper part of the landslide and seepage to the subsurface. This condition is favorable for creating high pore-water pressure. Finally, a combination of high pore pressures and additional water from the rainfall in the monsoon

season, causes the slope of Taprang landslide unstable in the future.

CONCLUSIONS

ERT was applied in the Taprang landslide to know the physical properties of soil and rock, subsurface lithology, groundwater condition, and geometry of the slip surface. The ERT data revealed the zones with a dry to saturated colluvial soil in the upper layer, highly saturated sandy to silty soil in the middle layer and bedrock of gneiss, schist, and quartzite in the bottom layer of different parts of the landslide. The resistivity sections also showed that bedrock is cracked, weathered, and fractured at some places. Highly sheared bedrock and lithology are present mainly in the body part of the landslide. Similarly, the groundwater zones were indicated by low resistivity value and lie at depths 10–25 m which is deeper in-depth at the crown area and slightly shallower in body part and toe of the landslide. The depth to slip surface varies from places and found at depth 25 m at the crown, 10–20 m at the main body part, and more than 50 m toward the toe area. This geometry of slip surface suggests the slip surface is curved and landslide movement is in rotational type.

Finally, the geophysical method (ERT) therefore, can be used for identifying subsurface lithological variation, geometry, and physical properties of soil and rock mass where other geotechnical studies

such boreholes and trenches are not feasible. The 2D inversion images with resistivity contrasts between the overburden deposit and the bedrock demarcated the geometry and slip surface of the landslide. In the future, this method could be used to investigate the landslide area continuously for the design of mitigating measures in the Taprang landslide as well as a similar landslide in Nepal.

ACKNOWLEDGEMENTS

We thank Vulnerable Landslide Management Project (VLMP), Government of Nepal for facilitating and funding this work through GOEC Nepal. We would like to thank the Department of Geology, Tri-Chandra Multiple Campus for providing support for this dissertation work to the second author. We would also like to thank Krishna Prasad Upadhyay, Senior Divisional Hydro-geologist GoN, and Shyam Prasad Adhikari, Alpine Consultancy Pvt. Ltd. for arranging necessary support for this work. We are also indebted to Suvash Acharya for his assistance during the fieldwork.

AUTHOR'S CONTRIBUTIONS

The geological field work was conducted by R.K. Adhikari under the supervision of A. Sigdel. All ERT profiles were prepared by A. Sigdel and the interpretation was done jointly by the authors and finalized for the manuscript. The paper was drafted by A. Sigdel and both authors read, discussed and approved for the publication.

REFERENCES

- Asriza, Supriyanto, T.H.W. Kristyanto, T.L. Indra, R. Syahputra, and A.S. Tempessy Asriza, Supriyanto, T.H.W. Kristyanto, T.L. Indra, R. Syahputra, and A.S. Tempessy Asriza, Supriyanto, T.H.W. Kristyanto, T.L. Indra, R. Syahputra, and A.S. Tempessy
- Asriza, S., Kristyanto T.H.W., Indra T.L., Syahputra R., and Tempessy A.S., 2017, Determination of the Landslide Slip Surface Using Electrical Resistivity Tomography (ERT) Technique. *Advancing Culture of Living with Landslides*, Springer International Publishing AG pp. 54-61.
- Batayneh, A.T., Al-Diabat, A.A., 2002, Application of a two-dimensional electrical tomography technique for investigating landslides along the Amman–Dead Sea highway, *Jordan Environmental Geology* v. 42, pp. 399–403.
- Bichler A., Bobrowsky P., Best M., Douma M., Hunter J., Calvert T., Burns R., 2004, Three-dimensional mapping of a landslide using a multi-geophysical approach: the Quesnel Forks landslide. *Landslides* v.1, pp. 29–40.
- Bogoslovsky V. and Ogilvy, A., 1977, *Geophysical Methods for the Investigation of Landslides, Geophysics*, v. 42, No. 3, pp. 562-571.
- Caris J.P.T., Van Asch Th W.J., 1991, Geophysical, geotechnical and hydrological investigations of a small landslide in the French Alps. *Engineering Geology*, v. 31, pp. 249-276.
- Coşkun, N., Çakır, Ö., Erduran, M. Kutlu YA., Cetinar ZS., 2016, A potential landslide area investigated by 2.5D electrical resistivity tomography: case study from Çanakkale, Turkey. *Arab J Geosci* 9, 6, <https://doi.org/10.1007/s12517-015-2026-x>
- Demoulin, A., Pissart, A., Schroeder, C., 2003, On the origin of late Quaternary palaeo landslides in the Liège (E Belgium) area. *International Journal of Earth Science*, v. 92, pp. 795–805.
- Department of Mines and Geology, 1983., *Geological Map of Western Central Nepal*. Scale 1: 250000.
- Dhital, M. R., 2015, *Geology of the Nepal Himalaya: Regional Perspective of the classical collided orogen*. Springer International Publication, Switzerland, pp. 230-233.
- Drahor, M.G., Gokturkler, G., Berge, M.A., Kurtulmus, T.O., 2006, Application of electrical resistivity tomography technique for investigation of landslides: a case from Turkey. *Environmental Geology*, v. 50, pp. 147–155.
- Epada P.D., Sylvestre G., Tabod T.C., 2012, Geophysical and Geotechnical Investigations of a Landslide in Kekem Area, Western Cameroon, *International Journal of Geosciences*, v.3, pp. 780-789.
- Jongmans D., Garambois, S., 2007, Geophysical investigation of landslides : a review *Bulletin Société Géologique de France, Société Géologique de France*, v. 178 (2), pp.101-112.
- Griffiths, D.H. and Turnbull, J., 1985. A multi-electrode array for resistivity surveying. *First Break* 3 (No. 7), pp.16-20.
- Hack, R., 2000. *Geophysics for slope stability. Surveys in geophysics*. v. 21, pp. 423–448.
- Havenith, H.B., Jongmans, D., Abdrakmatov, K., Trefois, P., Delvaux, D., Torgoev, A., 2000, Geophysical investigations on seismically induced surface effects, case study of a landslide in the Suusamyrvally, Kyrgyzstan. *Survey in geophysics* v.21, pp.349–369.
- Khanal N.R., Koirala A., Gurung S.B., Kumar U., Rijal R, Sigdel S., Acharya C., Yadav U.P., 2013, Madi River, Nepal: landslide dam outburst flood risk management. ICIMOD, Nepal.
- Kneisel C, Hauck C., 2008, Electrical method. In: Hauck C, Kneisel C(eds) *Applied geophysics in periglacial*

- environments. Cambridge University Press, Cambridge, pp 3–27.
- Konagai K., Numada M., Zaferiakos A., Johansson J., Sadr A., Katagiri T., 2005, An example of landslide-inflicted damage to tunnel in the 2004 Mid-Niigata prefecture earthquake, *Landslides* v. 2 pp. 159-163.
- Lapenna, V., Lorenzo, P., Perrone, A., Piscitelli, S., Rizzo, E., Sdao, F., 2003, High-resolution geoelectrical tomographies in the study of the Giarrossa landslide (Potenza, Basilicata), *Bulletin. Engineering. Geology and Environment* v.62, pp. 259–268.
- Lapenna, V., Lorenzo, P., Perrone, A., Piscitelli, S., Rizzo, E., Sdao, F., 2005, 2D electrical resistivity imaging of some complex landslides in Lucanian Apennine chain, southern Italy, *Geophysics* v.70, B11–B18.
- Loke M.H. and Barker R.D., 1996 a. Rapid least-squares inversion of apparent resistivity pseudo sections using a quasi-Newton method. *Geophysical Prospecting*, v.44, pp.131-152.
- Loke M H., 2009, Tutorial: 2-D and 3-D electrical imaging surveys www.geoelectrical.com.
- Loke M.H., 2014, Tutorial: 2-D and 3-D electrical imaging surveys. Geotomo Software, Malaysia.
- Loke, M.H., Dahlin, T., Rucker, D.F., 2014, Smoothness-constrained time-lapse inversion of data from 3D resistivity surveys. *Near Surface. Geophysics*.v.12, pp. 5–24.
- Palacky, G.V. 1987, Resistivity characteristics of geologic targets, in *Electromagnetic Methods in Applied Geophysics*, v. 1, Theory, 1351
- Pasierb B., 2012, Resistivity tomography in prospecting geological surface and anthropogenic objects. *Techn Trans Environ Eng* v. 23, pp 201–209.
- Pasierb B., 2015, Numerical Evaluation 2D electrical resistivity tomography for investigations of subsoil. *Techn Trans Environ Eng* 2-Š pp. 101–113.
- Ponziani M., Slob E.C., Ngan-Tillard D.J.M., Vanhala H., 2011, Influence of water content on the electrical conductivity of peat, *International Water Technology Journal, IWTJ* v.1, Issue, 1 pp.14-21.
- Regmi, A. Yoshida K., Cui P., Hatano N., 2017, Development of Taprang landslide, West Nepal, *Landslides*, v. 14, No. 3, pp.929-946
- Sassa, K., Tiwari, B., Liu, K.-F., McSaveney, M., Strom, A., Setiawan, H. (Eds.) 2018, *Landslide Dynamics: ISDR-ICL Landslide Interactive Teaching Tools. Volume 1: Fundamentals, Mapping and Monitoring.* Springer
- Suzuki. K., Higashi S., 2001, Groundwater flow after heavy rain in landslide-slope area from 2-D inversion of resistivity monitoring data, *Geophysics*, v. 66(3) pp. 707-984
- Stöcklin, J. and Bhattarai, K. D., 1977, *Geology of Kathmandu area and central Mahabharat range Nepal.* In: *Himalaya Report*, Department of Mines and Geology, Kathmandu, Nepal, 86 p.
- Telford W.M., Geldart LP., Dan Sheriff R.E., 1990, *Applied geophysics*, 2nd edn. Press Syndicate of the University of Cambridge, New York.
- Wightman, W. E., Jalinoos, F., Sirles, P., and Hanna, K. 2003, *Application of Geophysical Methods to Highway Related Problems.* Federal Highway Administration, Central Federal Lands Highway Division, Lakewood, CO, Publication No. FHWA-IF-04-021
- Yang C.H, Liu H.C., Lee C.C., 2004, Landslide investigation in the Li-Shan area using resistivity image profiling method. In: *SEG 74th annual meeting*, Denver, Colorado, 10–15 October 2004.